Collision-induced rototranslational spectra of H_2-Ar from an accurate *ab initio* dipole-moment surface

Wilfried Meyer
Fachbereich Chemie, Universität, 675 Kaiserslautern, Federal Republic of Germany

Lothar Frommhold
Physics Department, University of Texas at Austin, Austin, Texas 78712-1081
(Received 9 June 1986)

The induced dipole moment of hydrogen- (H_2) argon pairs is obtained with an estimated accuracy of about 2% by treating the collisional complex like a molecule in self-consistent-field (SCF) and coupled-electron-pair calculations. The basis-set superposition error is effectively avoided by the use of nonorthogonal local orbital sets. Based on the four-term, *ab initio*, orientation-dependent dipole function and a reliable isotropic potential model, the rototranslational absorption spectra of free and bound H_2-Ar pairs are computed from an exact quantum formalism. Both the spectral profile and absolute intensity of the *ab initio* spectra are shown to be in agreement with Dore and Birnbaum's recent measurement. The work demonstrates once more what was seen previously for the He-Ar and H_2-He far-infrared absorption spectra, namely that the precision attainable in such *ab initio* computations matches or exceeds that of the best available measurements of the same spectra [Meyer and Frommhold, Phys. Rev. A **33**, 3807 (1986), and Phys. Rev. A **34**, 2771 (1986).

I. INTRODUCTION

The atmospheres of the outer planets consist of hydrogen (H_2), with small admixtures of mostly infrared-inactive species such as He, CH_4, Ar, etc. In the infrared, the dominant spectral features thus arise from induced dipoles of collisional pairs, like H_2-He, H_2-H_2, etc. The experimental study of such collision-induced absorption (CIA) spectra is rather difficult at the temperatures encountered in planetary atmospheres, and the few existing laboratory measurements of such spectra have been taken at fixed temperatures, like 77.4 or 195 K. Therefore, for the study of these atmospheres, it is necessary to model the CIA spectra from theory. This requires the knowledge of the interaction potential and collision-induced dipole moment. While for the modeling of the interaction potential useful spectroscopic, scattering, bulk, etc., data usually exist, an accurate dipole moment function is best derived from *ab initio* calculations.

Theortical attempts to determine collision-induced dipole moments have been reviewed by Meyer.[1] So far, these have been restricted to the dissimilar pairs of noble-gas atoms and the molecular pairs H_2-He and H_2-H_2. Accurate *ab initio* dipole moments which include the effects of electron correlation have been communicated only recently for He-Ar (Ref. 2) and H_2-He (Ref. 3). The spectra computed on the basis of the *ab initio* dipole moment agree with the most dependable measurement within the estimated experimental accuracy of $\sim 10\%$. H_2-Ar is among the few collisional systems for which accurate CIA spectra have been measured.[4] These may serve to further probe the potential of theoretical predictions of the CIA spectra. Furthermore, the H_2-Ar system is of interest because argon has been suspected in planetary atmospheres. The H_2-Ar dipole moment function is also of interest for spectroscopic work with the bound H_2Ar van der Waals complex.[5]

In this work, we report the results of our *ab initio* calculations of the induced dipole moment components for various H_2-Ar separations and H_2 orientations at the vibrationally averaged H—H bond distance. We will also construct an analytical representation of the dipole moment function, obtain theoretical rototranslational CIA spectra based on an advanced semiempirical, isotropic interaction potential, and compare these with an available measurement.

II. *Ab initio* DIPOLE MOMENT FUNCTION

The problems encountered in *ab initio* calculations of the typically small induced dipole moments of collisional complexes have been discussed in detail in previous work on He-Ar (Ref. 2), H_2-He (Ref. 3), and H_2-H_2 (Ref. 6). The present H_2-Ar calculations follow closely the procedures used for H_2-He which are described elsewhere.[1,3] These may be summarized as follows. (1) Subsequent to a self-consistent-field (SCF) calculation, the orbitals are transformed to a localized form, in order to ascribe these to one or the other collisional partner, to obtain a basis for separating the intraspecies and interspecies correlation effects. (2) In a multiconfigurational (MC) SCF calculation, the wave function is then augmented by the leading H_2 double substitutions $1\sigma_g^2 \rightarrow 1\sigma_u^2$, $1\pi_u^2$, and $2\sigma_g^2$, in order to account for the static multipole moments of H_2 adequately (e.g., the H_2 quadrupole moment is thereby reduced by 10% relative to the SCF value). (3) Electron correlation is further included by considering all single and double substitutions of the above-defined MC function in a size-

TABLE I. Pertinent properties of Ar, H_2, and H_2-Ar at long range, in a.u.

		SCF	CEPA	Accurate
Ar	α	10.51	10.88	11.067[a]
H_2	$\alpha_{\parallel}$	6.773	6.765	6.766[b]
	$\alpha_{\perp}$	4.762	4.714	4.752[b]
	q_2	0.525	0.480	0.485[b]
	q_4	0.359	0.333	0.353[b]
H_2-Ar	B_{23}[c]	9.70	9.20	9.29[a,b]
	B_{45}[c]	9.82	10.12	11.18[a,b]

[a]A. Dalgarno and A. E. Kingston, Proc. R. Soc. London, Ser. A **259**, 424 (1960).

[b]W. Kolos and L. Wolniewicz, J. Chem. Phys. **46**, 1426 (1967); G. Karl, J. D. Poll, and L. Wolniewicz, Can. J. Phys. **53**, 1781 (1975); J. D. Poll and L. Wolniewicz, J. Chem. Phys. **68**, 3053 (1978).

[c]Obtained by fitting the long-range part of the calculated dipole moment function.

consistent, coupled-electron-pair approximation (CEPA-1, Ref. 7). (4) At this level, basis-set superposition errors are effectively avoided by restricting the orbital space used for intrafragment correlation to the basis functions belonging to a particular collisional partner. This is readily implemented by using the self-consistent electron pairs technique[8,9] (SCEP) which allows the use of different orbital sets for different electron pairs.

The basis sets of Gaussian-type orbitals (GTO's) employed for Ar and H_2 are identical with the ones used previously in the He-Ar and H_2-He calculations,[2,3] respectively. Care has been taken that properties which determine the induced dipole moments, namely the static multipole moments of H_2, the dipole polarizabilities of Ar and H_2, and the extensions of their electron distributions, are accurately accounted for. From the results shown in Table I, we conclude that at large separations the specified wave function factors properly and describes adequately the correlated fragments. From these data, and on the basis of our experience with similar dipole moment calculations for stable molecules,[10–12] we estimate that the uncertainty of our H_2-Ar dipole results are in the order of 2%.

All calculations have been performed for the mean bond length of hydrogen, $\langle r_{HH} \rangle = 1.449$ bohr.[13] This r-centroid approximation effectively accounts for zero-point vibrational averaging. At long range, this is quite obvious from the information given in Table I, and at short range we refer to the H_2-He results:[3] Although the exchange terms as functions of r_{HH} show a considerable curvature, the dipole moments calculated at the mean bond length were smaller by a mere 2% than those obtained from a vibrational average of a quadratic dipole function. Certainly, for H_2-Ar, this difference is even smaller because in the critical range around the collision diameter, the dipole moment is more clearly dominated by the induction terms, due to the much larger Ar polarizability.

For each interfragment separation, dipole moments have been calculated for three orientations of H_2, namely at the angles 0°, 45°, and 90° between the interfragment and hydrogen axes. This allows a determination of the four leading terms in the usual expansion of the dipole moment function,[14,15]

$$\mu_M(\mathbf{r},\mathbf{R}) = \frac{4\pi}{\sqrt{3}} \sum_{\lambda,L} A_{\lambda L}(r,R) \sum_m C(\lambda L\, 1; m, M-m) \times Y_\lambda^m(\hat{\mathbf{r}}) Y_L^{M-m}(\hat{\mathbf{R}}) \,. \quad (1)$$

In this expression, the vector $\mathbf{r}$ connects the protons of H_2 and $\mathbf{R}$ connects Ar with the center of H_2; $\hat{\mathbf{r}}$ and $\hat{\mathbf{R}}$ are the corresponding unit vectors while r and R denote the norms of $\mathbf{r}$ and $\mathbf{R}$, respectively. We note that for molecules with inversion symmetry, the expansion parameter λ must be even. From the Clebsch-Gordan coefficient, Eq. (1), it follows that the expansion parameter L differs by no more than ± 1 from λ; L is an odd integer. At long range, one finds[14]

$$A_{\lambda,\lambda+1} = \alpha q_\lambda \sqrt{\lambda+1} R^{-\lambda-2}, \quad A_{\lambda,\lambda-1} = 0 \,, \quad (2)$$

TABLE II. Calculated dipole moments in 10^{-6} a.u. (CI stands for configuration interaction).

	R	$\mu_z(0°)$	$\mu_z(90°)$	$\mu_z(45°)$	$\mu_x(45°)$
CI	5.0	60 717	−3244	25 851	−7912
	5.5	32 891	−5415	12 223	−6709
	6.0	18 900	−5272	6001	−5336
	7.0	7764	−3487	1874	−3179
	8.0	4074	−2077	893	−1906
	9.0	2463	−1268	547	−1210
SCF	5.0	68 297	+601	31 771	−7884
	5.5	37 620	−3195	15 759	−6752
	6.0	21 820	−4038	8092	−5405
	7.0	8871	−3166	2588	−3261
	8.0	4526	−2034	1143	−1979
	9.0	2683	−1278	655	−1258
Intramolecular CI	5.5	36 419	−3862	15 052	−5999
	9.0	2560	−1223	620	−1211

where α designates the argon polarizability and q_λ a multipole moment of H_2; for example, q_2 designates the hydrogen quadrupole moment. The short-range exchange and distortion contributions are expected to behave approximately as an exponential function of R, similar to the exchange repulsion energy.[16,17] Vibrational averaging yields the dipole expansion coefficients

$$B_{\lambda L}^{vv'}(R)=\langle v' \mid A_{\lambda L}(r,R) \mid v \rangle \ . \tag{3}$$

Since we assume a linear variation of the expansion parameters $A_{\lambda L}(r,R)$ over the range of vibrational motion, in the r-centroid approximation for the vibrational ground state ($v=v'=0$), we have

$$B_{\lambda L}^{00}(R)\simeq A_{\lambda L}(\langle 0 \mid r \mid 0 \rangle,R) \ , \tag{4}$$

with $\langle 0 \mid r \mid 0 \rangle = \langle r_{HH} \rangle = 1.449$ bohr.

The calculated dipole moments are collected in Table II and the expansion coefficients $B_{\lambda L}^{00}$ are given in Table III. The latter are also displayed in Fig. 1. As expected from the large Ar polarizability, the quadrupole induced term B_{23}^{00} is dominant over the whole range considered. At the collision diameter, this term deviates from the pure long-range expression, Eq. (2) and dashed curve marked $23l$ in Fig. 1, by $+13\%$, due to overlap effects which are negligible at long range. This overlap contribution affects the absorption intensities considerably more than the pure overlap terms B_{01}^{00} and B_{21}^{00} owing to the interference with the strong long-range part.

For a more complete documentation, and also in order to indicate the effects of electron correlation, we include in Table II the dipole moments obtained at the SCF level and, for two fragment separations, also those which result when only intrafragment correlation is considered. The correlation effects on the leading terms B_{01}^{00} and B_{23}^{00} are given in Table IV for these two separations. As in the case of H_2-He, intrafragment correlation affects the coefficient B_{23}^{00} in a way as if the H_2 quadrupole moment were reduced by 9% and the Ar polarizability increased by 2%. Somewhat surprisingly, correlation does not increase B_{01}^{00} at shorter distances, in contrast to the effect found for Ar-He.[2] On the other hand, interfragment correlation reduces B_{01}^{00} considerably ($\sim 30\%$ at 5.5 bohr), on account of the rather large dispersion force in H_2-Ar.

For a convenient calculation of the spectral profiles, an analytical form of the expansion coefficients $B_{\lambda L}^{00}$ is desirable. The numerical results can be described quite accurately by a function of the form

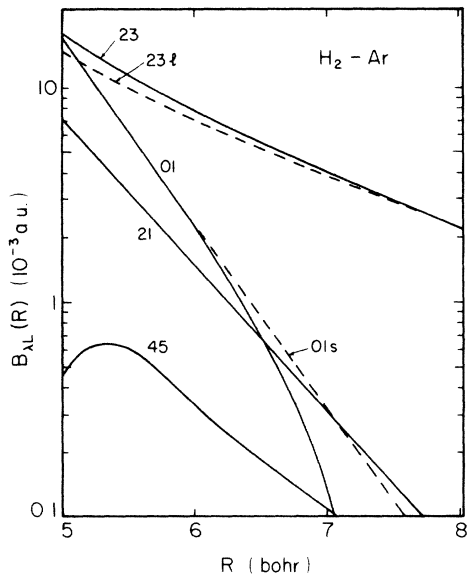

FIG. 1. Induced dipole moment components as function of separation, in atomic units. Curves are labeled λL; the letters l and s indicate pure long- and short-range parts, respectively. (1 a.u. $=8.478\times10^{-30}$ C m.)

$$B(R)=B^{(n)}R^{-n}+B^{(0)}\exp[a(R-R_0)+b(R-R_0)^2] \tag{5}$$

which is a slight generalization of the functional form used by van Kranendonk;[14] subscripts λL will be attached to the B coefficients as needed. The value of $R_0=6.0$ bohr has been chosen to be close to the collision diameter so that $B^{(0)}$ gives in essence the size of the exchange and distortion dipole contribution at the collision diameter. $B^{(n)}$ accounts for the long-range induction or dispersion contributions, with the value of n taken from the leading term of this kind. It should be noted that the fit parameter $B^{(n)}$ comprises contributions from higher-order terms that are effective at distances from 7 to 9 bohr while the damping of the long-range terms, which is relatively large only for the dispersion term, is absorbed in the second term of Eq. (5). The parameters of the fit are collected in Table V. The input values of Table IV are reproduced with an accuracy of better than 1%. As noted above, the long-range coefficient $B_{23}^{(4)}$ obtianed from this fit is in excellent agreement with the value expected from the accurately known properties of the separated systems (compare Table II) and even the much smaller $B_{45}^{(6)}$ is reasonably consistent with it.

TABLE III. Dipole moment expansion coefficients in 10^{-6} a.u.

R (bohr)	B_{01}^{00}	B_{23}^{00}	B_{21}^{00}	B_{45}^{00}
5.0	16537	17893	−7460	1179
5.5	6545	11666	−3362	619
6.0	2351	7897	−1504	332
7.0	122	4018	−311	108
8.0	−82	2281	−77	42
9.0	−51	1411	−17	20

TABLE IV. Correlation effects on the leading terms B_{01}^{00} and B_{23}^{00} in 10^{-6} a.u.

	B_{01}^{00} ($R=5.5$ bohr)	B_{23}^{00} ($R=5.5$ bohr)	B_{01}^{00} ($R=9.0$ bohr)	B_{23}^{00} ($R=9.0$ bohr)
$\sqrt{3}\alpha q_2$		10160		1416
SCF	9635	12279	15	1485
SCF + intramolecular CI	8911	11847	12	1425
SCF + intramolecular and intermolecular CI	6545	11666	−51	1411

TABLE V. Fit parameters of the $B^{00}_{\lambda L}$, Eq. (10), (with $R_0=6.0$ bohr), in a.u.

λ	L	n	$B^{(n)}$	$B^{(0)}$	a	b
0	1	7	−278.846	0.003 344 4	−1.888	−0.094
2	3	4	9.199	0.000 798 9	−1.422	−0.041
2	1	0	0.000	−0.001 500 6	−1.575	0.032
4	5	6	10.126	0.000 116 1	−1.576	−0.057

Table VI presents the SCF and CI interaction energies. As is generally the case in CI calculations with a finite basis, the dispersion attraction is underestimated considerably. A defect of about 15% around the minimum of the potential leads to a well depth which is only $\frac{2}{3}$ of that deduced from spectroscopic information.[8] The root of the isotropic potential is calculated at 6.16 bohr while the semiempirical root is only 6.0 bohr. It is interesting to note that the calculated isotropic potential intercepts the semiempirical one at about 5 bohr, in spite of the systematic defect of the attraction. This indicates that the latter potential is likely to be too repulsive for distances shorter than 5.5 bohr. The SCF energies are in satisfactory agreement with Tang and Toennies's repulsive energies derived from their semiempirical potential model.[18] The anisotropy of the theoretical potential, which is usually less affected by the defect of the dispersion forces, is in reasonable agreement with the semiempirical anisotropy. In the well region, the calculated anisotropy is slightly smaller than that of LeRoy *et al.*[19] deduced from spectroscopic data; it nearly coincides with that of Reuss and Zandee based on scattering experiments.[20] On the other hand, in the repulsive region it rises more steeply with decreasing separations R than the latter potential and supports the stronger anisotropy derived by LeRoy.[18,19]

TABLE VI. Interaction energies (10^{-6} hartree).

R (bohr)	0°	90°	45°
5.0	7275[a]	5514[a]	6343[a]
	5223[b]	3613[b]	4118[b]
5.5	2995[a]	2261[b]	2609[a]
	1675[b]	1096[b]	1359[b]
	3293[c]	3263[c]	2791[c]
6.0	1209[a]	910.8[a]	1053[a]
	370.0[b]	194.7[b]	272.6[b]
7.0	187[a]	140.1[a]	162.9[a]
	−150.9[b]	−136.3[b]	−144.7[b]
8.0	26.9[a]	19.6[a]	23.1[a]
	−117.1[b]	−94.1[b]	−105.6[b]
9.0	2.9[a]	2.2[a]	
	−63.2[b]	−47.9[b]	

[a]SCF.
[b]CEPA-1, intermolecular + intramolecular CI.
[c]CEPA-1, intramolecular CI only.

III. ROTOTRANSLATIONAL SPECTRA

Collision-induced dipole spectra of the H_2-Ar complex have been measured in the forbidden rotational,[4] fundamental, and overtone[5] hydrogren bands as the enhancement over the CIA H_2-H_2 spectra arising from the addition of argon. As a test of the induced dipole data, we will compute the rototranslational spectra of H_2-Ar in the far infrared, near the hydrogen rotational lines $S_0(J)$, $J=0,1,2,\ldots$, for comparison with the recent measurements of Dore and Birnbaum,[4] using a rigorous line-shape formalism discussed elsewhere.[21]

A meaningful computation of a spectral line shape requires a potential model which describes the interactions accurately at close range, roughly where the separation R is comparable to the collision diameter σ. Since the anisotropy of the H_2-Ar interaction is small, we use the isotropic potential approximation, an enormous simplification of the line-shape computations.[21,22] Recent investigations by Schäfer[23] and Moraldi *et al.*[24] have indicated that the anisotropy of the H_2-He interaction potential, which is comparable to that of the H_2-Ar pair, affects CIA line shapes discernibly only in the far wings which are here of lesser interest. For our work, we choose the isotropic part of the BC3 potential[19] which is one of the most advanced H_2-Ar potential models presently available. It is of the Buckingham-Corner form, with dispersion damping at near range. It is based on spectroscopic and reliable theoretical data at near and distant range. It is also consistent with beam scattering data.[19,25]

The results of the line-shape computations are shown in Fig. 2. The isotropic overlap-induced component, $\lambda L=01$, is relatively weak and significant only at low frequencies. This is in striking contrast to the case of the analogous H_2-He spectra where the 01 component is relatively prominent, see Figs. 2 and 3 of Ref. 21. However, we note that on an absolute intensity scale, the 01 components of H_2-He and H_2-Ar are of similar magnitude, and the real difference between the spectra of the two systems is related to the high polarizability of argon which for the pair H_2-Ar enhances the rotational H_2 lines by almost 2 orders of magnitude. In fact, the quadrupole-induced component of H_2-Ar completely determines the appearance of the spectra and differs from the total only at low frequencies, where the 01 component is of comparable magnitude (dashed curves). The anisotropic 21 component amounts to less than 2% of the total intensity everywhere, and the 45 component is even less important except at the highest frequencies where feeble U lines ($\Delta J=4$) occur (not shown).

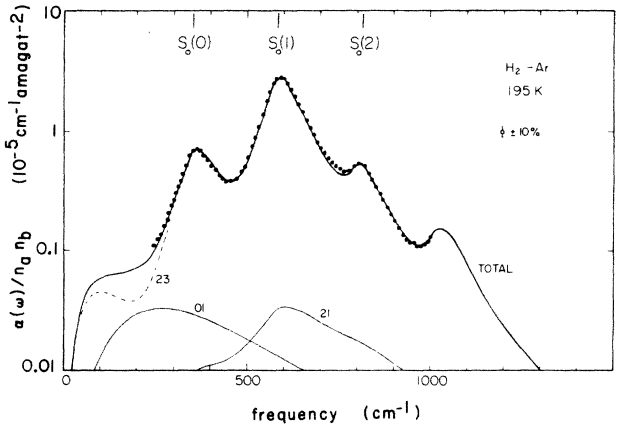

FIG. 2. Rototranslational absorption coefficient $\alpha(\omega)$ of H_2-Ar at 195 K. The position of the forbidden rotational hydrogen lines, $S_0(J)$ with $J=0$, 1, and 2, are shown. Components $\lambda L=01$ and 21 are sketched lightly; the 23 component is shown (dashed) only where it is different by more than a few percent from the sum of the 01, 21, and 23 components (marked total). Dots represent Dore and Birnbaum's measurement (Ref. 4). We note that the spectroscopic features of the van der Waals dimers, which occur near the peaks of the rotational hydrogen lines, have in this figure been flattened by convoluting the dimer contributions with a triangular slit function of 10 cm^{-1} full width at half maximum.

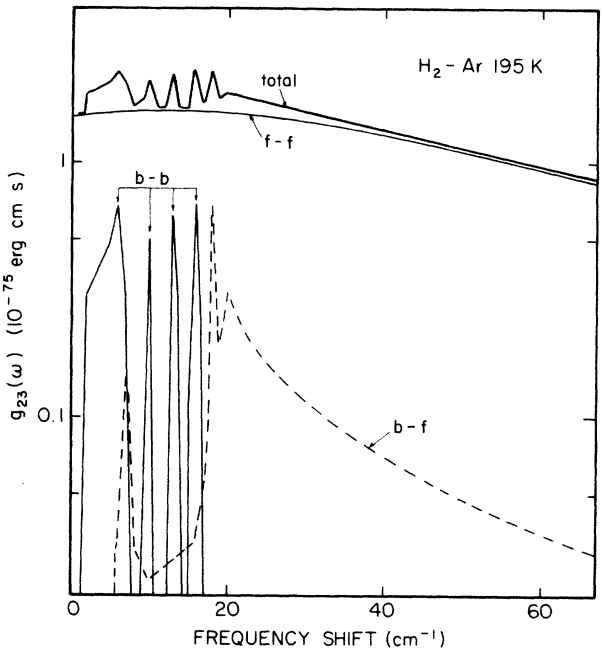

FIG. 3. The spectral function $g_{23}(\omega)$ at small, positive frequency shifts ("blue wing"). The spectral components arising from free-free (f-f), bound-bound (b-b), and bound-free and free-bound (b-f) transitions, as well as their sum (marked "total"), are given. The bound-bound features are here convoluted with a triangular slit function of 1 cm^{-1} full width at half maximum.

We note that the H_2-Ar complex forms dimers. Therefore, for the computation of the spectra, we consider bound as well as free complexes of H_2-Ar. The free-free transitions of H_2-Ar pairs are superimposed with bound-free and bound-bound components as the excellent measurements of Welsh and associates have shown.[26–28] However, such dimer spectra are known from observation only in the fundamental and overtone bands of hydrogen. Theory indicates their presence also in the pure rotational lines.[22,29,30] These have as yet not been seen in the laboratory, presumably because of the low resolution ($\gtrsim 10$ cm^{-1}) and high densities ($\gtrsim 40$ amagats) typically employed. These dimer spectra will be described next.

With the BC3 intermolecular potential model[19] in the isotropic potential approximation, the H_2-Ar dimer features six rotational levels ($l=0,\ldots,5$) in the vibrational ground state ($v=0$), one rotational level ($l=0$) in the vibrationally excited state ($v=1$), and three prominent scattering resonances at $l=6$, 7, and 8 which may be considered an extension of the rotational levels of the ground state ($v=0$). For each λL component, we have a specific dimer spectrum near zero frequency, and also around the centers of the rotational hydrogen $S_0(J)$ lines. Of these, only the $\lambda L=23$ component is significant near the centers of the $S_0(J)$ lines. For this component, the selection rules are $\Delta l=\pm 1,\pm 3$. The bands with $\Delta l=+1$ and $+3$ appear at positive frequency shifts, and the $\Delta l=-1,-3$ bands at negative frequency shifts relative to the line centers of the hydrogen $S_0(J)$ lines [354 and 587 cm^{-1} for $S_0(0)$ and $S_0(1)$, respectively].

Figure 3 shows a computed dimer spectrum. The spectral function $g_{23}(\omega)$ is plotted, which is related to the absorption coefficient $\alpha(\omega)$ according to[21]

$$\alpha(\omega)\simeq\frac{4\pi^2}{3\hbar c}n_a n_b\omega\left[1-\exp\frac{-\hbar\omega}{kT}\right]\times\sum_{J,J'}(2J+1)P_J g_{23}(\omega-\omega_{JJ'}) \tag{6}$$

in the vicinity of the rotational $S_0(J)$ lines of hydrogen. The $\omega_{JJ'}$ are the hydrogen rotational transition frequencies. We see that for a given rotational line $S_0(J)$, the spectral function g_{23} and absorption coefficient α are practically proportional over the small-frequency band shown in Fig. 3. Only positive frequency shifts, i.e., upward transitions, are shown. Downward transitions occur at negative frequency shifts and the spectrum shown in Fig. 3 must be supplemented by its approximate mirror image, with intensities slightly adjusted at negative shifts according to the principle of detailed balance.[21] Besides the transitions from free states to other free states (labeled f-f), the bound-to-bound (b-b) and bound-to-free and free-to-bound (b-f) transitions are shown; all bound-bound lines are convoluted with a triangular slit function of 1 cm^{-1} full width at half maximum.

The $\Delta l=+1$ band consists of four bound-bound lines at 2.2, 3.3, 4.4, and 5.3 cm^{-1}, plus three bound-free lines at 6.1, 6.8, and 7.4 cm^{-1} involving the predissociating dimer states with $l=6$, 7, and 8. All of these lines are not resolved but their envelopes are discernible at small fre-

quency shifts. The $\Delta l = +3$ band, on the other hand, consists of three lines at 6.7, 9.9, and 13 cm^{-1} (b-b), plus three bound-free transitions at 15.9, 18.2, and 20 cm^{-1}. These are discernible in the figure. Vibrational dimer transitions are not significant. At higher frequency shifts >20 cm^{-1}, an unstructured bound-free continuum is observed with an intensity of initially $\sim 20\%$ of the free-free contribution at 20 cm^{-1} shift. With increasing frequency shift, this continuum falls off faster than the free-free component and is insignificant at a shift of ~ 60 cm^{-1} or more. The intensities arising from transitions involving dimer states amount to almost 20% at the centers of the hydrogen $S_0(J)$ lines when convoluted with an instrumental profile of 10 cm^{-1} or more half width. Such convolution flattens essentially all dimer structures and demonstrates that the dimer contributions to the CIA spectra are significant, even at low resolution.

Summarizing, the comparison of the *ab initio* spectra with the measurement (dots, Fig. 2) is very satisfactory once the theoretical dimer structures are flattened by simulating low spectral resolution. We note that the comparison, Fig. 2, is on an absolute intensity scale and no adjustable parameters have been used anywhere.

IV. CONCLUSION

As observed previously for the collision-induced dipoles of the He-Ar and H_2-He systems,[2,3] the dipole moment of the H_2-Ar pair can be obtained accurately from the fundamental theory using state-of-the-art quantum-chemical computational procedures. When the *ab initio* dipole data are employed for a computation of the rototranslational CIA profiles both, intensity and shape agree with the measurement.[4] Since spectral intensities are proportional to the square of the dipole moment, the observed agreement within the estimated experimental uncertainty of $\sim 10\%$ would suggest that the computed dipole strengths are accurate to better than 5%. Our theoretical estimate suggests an even better accuracy ($\pm 2\%$) of the computed dipole strengths. In conjunction with an accurate interaction potential, the theoretical dipole components obtained here permit the computation of rototranslational CIA spectra of H_2-Ar which are at least as accurate as the best measurements of such spectra presently available. This fact is of interest for the modeling of planetary atmospheres for which CIA spectra need to be known at a variety of temperatures which usually differ from those of the existing laboratory measurements.

The work also predicts the (low-resolution) rotational spectra of H_2Ar van der Waals dimers which have hitherto not been observed in the laboratory in rototranslational spectra. Similar dimer spectra are also expected in the microwave region.

ACKNOWLEDGMENTS

We are grateful to Dr. P. Dore and Dr. G. Birnbaum who kindly made the measurement[4] available for the comparison with the fundamental theory prior to publication. The work is supported by the National Science Foundation, Grant No. AST-8310786. The support of the Deutsche Forschungsgemeinschaft, Sonderforschungsbereich No. 91, during the stay of L.F. at Kaiserslautern, is also acknowledged.

[1] W. Meyer, in *Phenomena Induced by Intermolecular Interactions,* edited by G. Birnbaum (Plenum, New York, 1985).
[2] W. Meyer and L. Frommhold, Phys. Rev. A **34**, 632 (1986).
[3] W. Meyer and L. Frommhold, Phys. Rev. A **34**, 2771 (1986), this issue.
[4] P. Dore and G. Birnbaum (unpublished).
[5] H. L. Welsh, in *Spectroscopy,* Ser. 1, Vol. 1 of *Physical Chemistry,* edited by A. D. Buckingham and D. A. Ramsay (Butterworths, London, 1972).
[6] W. Meyer, L. Frommhold, and G. Birnbaum (unpublished).
[7] W. Meyer, in *Methods of Electronic Structure Theory,* edited by H. F. Schaefer III (Plenum, New York, 1978), Vol. IIIa, p. 413.
[8] W. Meyer, J. Chem. Phys. **64**, 2901 (1976).
[9] W. Meyer, R. Ahlrichs, and C. Dykstra, in *Advanced Theories and Computational Approaches to the Electronic Structure of Molecules* (Reidel, Dortrecht, 1984).
[10] W. Meyer and P. Rosmus, J. Chem. Phys. **63**, 2356 (1975).
[11] W. Meyer, P. Botschwina, P. Rosmus, and H. J. Werner, in *Computational Methods in Chemistry,* edited by J. Bargon (Plenum, New York, 1980), and references therein.
[12] P. Botschwina, Chem. Phys. **81**, 73 (1983).
[13] W. Kolos and L. Wolniewicz, J. Chem. Phys. **41**, 3663 (1964); **43**, 2429 (1965).
[14] J. D. Poll and J. van Kranendonk, Can. J. Phys. **39**, 189 (1961).
[15] J. D. Poll and J. L. Hunt, Can. J. Phys. **54**, 461 (1976).
[16] A. D. Buckingham, *Proprietes Optiques et Acoustiques de Fluids Comprimes et Actions Intermoleculaires* (Centre de la Recherche Scientifique, Paris, 1959), p. 57.
[17] A. D. Buckingham, Adv. Chem. Phys. **12**, 107 (1967).
[18] K. T. Tang and J. P. Toennies, J. Chem. Phys. **74**, 1148 (1981).
[19] R. J. LeRoy and J. S. Carley, Adv. Chem. Phys. **42**, 353 (1980).
[20] L. Zandee and J. Reuss, Faraday Discuss. Chem. Soc. **62**, 304 (1977).
[21] G. Birnbaum, S. I. Chu, A. Dalgarno, L. Frommhold, and E. L. Wright, Phys. Rev. A **29**, 595 (1984).
[22] J. Borysow and L. Frommhold, in *Phenomena Induced by Intermolecular Interactions,* edited by G. Birnbaum (Plenum, New York, 1985).
[23] J. Schäfer (private communication).
[24] M. Moraldi, A. Borysow, J. Borysow, and L. Frommhold, Phys. Rev. A **34**, 632 (1986).
[25] G. C. Maitland, M. Rigby, E. B. Smith, and W. A. Wakeham, *Intermolecular Forces—Their Origin and Determination* (Clarendon, Oxford, 1981).
[26] A. Kudian, H. L. Welsh, and A. Watanabe, J. Chem. Phys. **43**, 3397 (1965).
[27] A. Kudian, H. L. Welsh, and A. Watanabe, J. Chem. Phys. **47**, 1190 (1967).
[28] A. Kudian and H. L. Welsh, Can. J. Phys. **49**, 230 (1971).
[29] L. Frommhold, R. Samuelson, and G. Birnbaum, Astrophys. J. **283**, L79 (1984).
[30] A. Borysow and L. Frommhold, Astrophys. J. **303**, 495 (1986); **304**, 849 (1986).